A CRUSTAL MODEL FROM GRAVITY INVERSION IN KARAKORUM

C. Braitenberg and R. Drigo
Department of Earth Sciences, University of Trieste
Via Weiss 1, 34127 Trieste, Italy. Fax +39-40-575519
e-mail: berg@univ.trieste.it

Abstract
The Bouguer gravity field in the Karakorum-Kohistan-Hindu Kush area shows extraordinary excursion in amplitude suggesting a complex crustal and lithospheric structure. We apply spectral methods in the analysis of the gravity field using existing data furnished by BGI (Bureau Gravimetrique International). We separate the long and medium to short wavelength part of the field in order to model mass anomalies located at different depths. The long wavelength part is inverted at Moho level and interpreted as Moho undulations. We obtain depths ranging from 40 km South of the MBT (Main Boundary Thrust) to 70 km in Karakorum and Hindu Kush. The residual field, or medium to short wavelength component of the field contains striking anomalies aligned with the major tectonic lines, the MMT (Main Mantle Thrust) and the MKT (Main Karakorum Thrust). The gravity inversion attributes these anomalies to mid crust and superficial anomalous masses, which must be taken into account when studying the local stress field.

Introduction

The topic of the present study is the inversion and interpretation of existing, publicly accessible gravity data across the Kohistan Arc, in NW-Pakistan. The region is set between the northern boundary of the Indian, and the southern boundary of the Eurasian plates.

The gravity inversion method furnishes an important tool in the study of the crustal structure in this area, which has been determined by seismic methods in only restricted areas (Beloussov et al., 1983). The results obtained from the seismic methods are integrated in the gravity inversion procedure. We apply an inversion process which combines a spectral with a classical approach. The gravity field is used for modelling the undulation of clear realistic density boundary layers, as the crust-mantle interface. The gravity contribution of the undulation of density boundary layers set at different depths mainly affects different parts of the gravity spectrum. This implies that filtering processes of the gravity field greatly divides the contribution of deep and superficial density boundaries. The most important deep density-boundaries are the Moho-discontinuity and the lithosphere-asthenosphere boundary. Of these, the undulation of the Moho gives the greatest contribution, due to its more than 10-fold density contrast (0.45 against 0.03 g/cm^3). Furthermore the lithosphere gravity effect is reduced owing to its greater depth. We use the results from lithosphere flexure models to estimate the lithospheric thickness and the resulting gravity contribution. The high frequency component of the gravity field across the Kohistan Arc shows a remarkable amplitude in variation, and we interpret this in terms of mid-crustal to superficial crustal inhomogeneities.

The inversion method we use has been applied profitably in the European Alps, where the results for crustal thicknesses could be tested and verified with the depths obtained from DSS at some checkpoints and seismological investigations, giving an excellent agreement between the different methods (Braitenberg et al., 1997). The study of the Karakorum range is divided into two problems, the first concerning the inversion of the regional gravity field, the second the residual more local field, which nonetheless presents a variation of over 160 mGal amplitude.

Owing to its extremely high Bouguer anomaly values (exceeding -550 mGal) the area of NW-Himalayas is a very interesting region to study with the gravimetric method. Succesively to the pioneering works of Bouguer in the 18th century and Airy and Pratt in the 19th century, there have been several studies concerned with the development of large scale Bouguer and Airy gravity maps, and Airy crustal root maps (McGinnis 1970, 1971; Marussi 1976, 1983; Farah et al. 1977; Ebblin 1983). New data acquisition and the study of the crustal thickness and structure of North-Western Pakistan along two profiles cutting the Kohistan arc was carried out by Ebblin (1983) and Malinconico (1986; 1989).

Verma and Prasad (1987) compiled and interpreted the observed Bouguer gravity anomaly in terms of Moho depth and density contrast between crust and mantle. The DSS (Deep Seismic Sounding) profiles shot as part of the Indo-Soviet Geodynamics project (Beloussov et al., 1983) was used to estimate crustal velocity values.

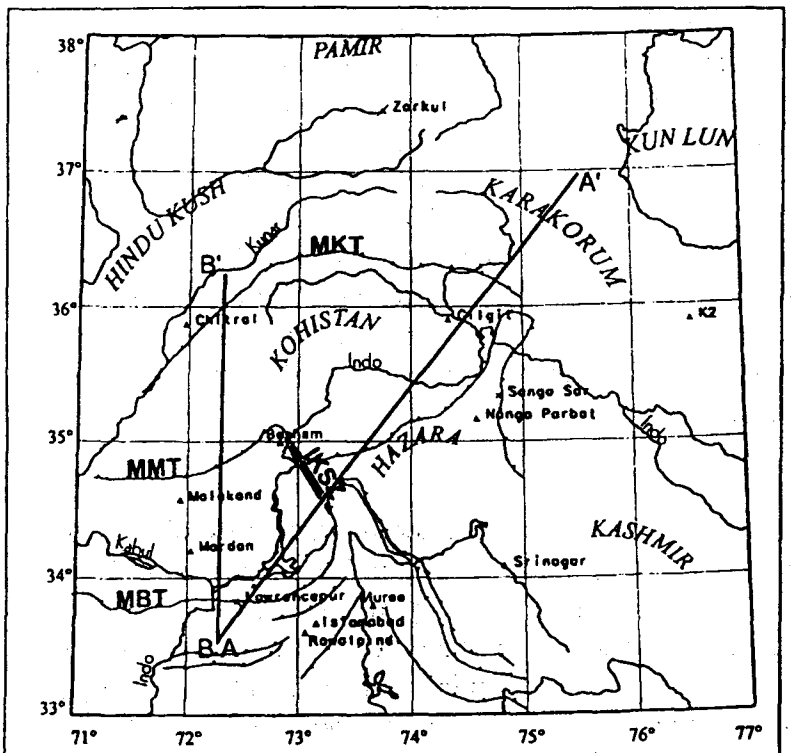

Fig. 1 Main tectonic provinces of Kohistan and surrounding areas. The line IKSZ marks the Indus-Kohistan seismic zone. The two profiles studied AA' and BB' have been added to the graph

A lithospheric flexure model of the Himalayan foreland in Pakistan has been developed by Duroy et al. (1989), incorporating gravity data along a NS profile extending southwards of Kohistan. The flexural rigidity of the plate and the boundary conditions on the bending moment and vertical shear stress were determined by fitting model anomalies to the observed Bouguer anomalies. The Indian plate is treated as an elastic plate, which is assumed to overlie a buoyant "fluid", and is flexed down under the weight of the overthrust mountains and the sediments eroded off the mountains and deposited in the foredeep basin. The model extends southward of the MMT, thus only marginally touching our region of study. Nevertheless the model predicts that the Moho dips northward at an angle of about 15° north of the MMT beneath the Kohistan Arc, starting from a depth of approximately 45 km.

A successive study of the flexure of the lithosphere in response to the topographic load was accomplished by Caporali (1995). The lithosphere is modelled as a thin, elastic, semi-infinite plate buoyant on a denser, inviscid fluid. The deformation of the plate is estimated by least squares reduction of the discrepance between modelled and observed Bouguer anomalies. The plate is assumed to be separated into an Indian and Asian portion.

Geological setting

The studied area belongs to the NW-Himalaya Ranges of Northern Pakistan. Geographically it is delimited by the Latitude 34°-37°, Longitude 70°-80°. In Pakistan the

Himalayan collision zone bends at approximately right angle from a NW-SE trending in the Himalayan range to a NE-SW direction of the Hindu Kush-Pamir. The Karakorum range forms the link between the NW-Himalaya to the East and the Hindu Kush and Pamir in the West and Northwest, respectively (Fig. 1).

Three important tectonic lines demarcate geologic boundaries, the Main Karakorum Thrust (MKT), the Main Mantle Thrust (MMT), and the Main Boundary Thrust (MBT). The MKT and the MMT (also termed Northern and Indus Sutures, respectively), separate the Kohistan-Ladakh Arc from the Indian plate to the South and the Asian plate to the North. The Kohistan sequence has been interpreted (Tahirkeli et al., 1983; Coward et al., 1986) as the crust and mantle of an obducted island arc (Fig. 2). The northern spur of the MBT is termed the NW Himalayan Syntaxis. Departing from the northern edge of the syntaxis and reaching the western bend of the MMT a NW-trending seismic line has been found by Armbruster et. al. (1978), termed the Indus Kohistan Seismic Zone (IKSZ). The microseismicity and the macroseismicity seem to occur on northeast dipping thrust faults. The broad seismic zone extends to 70 km depth. Up to now no geologic evidence of the IKSZ has been found.

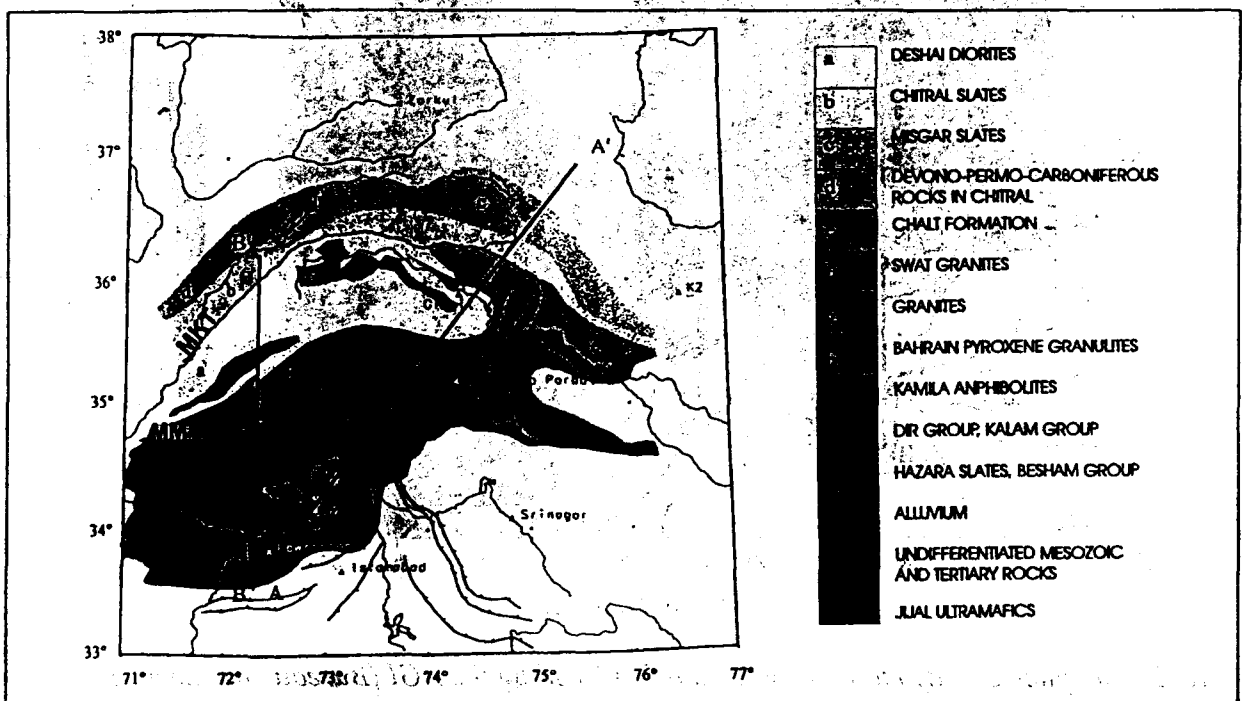

Fig. 2 Geologic map of the studied area (Tahirkheli, 1983). Main tectonic lines are the MKT, the MMT and the MBT. AA' and BB' are the two profiles we study in the gravity inversion

Gravity data

In Fig. 3 the Bouguer gravity anomaly map is shown, based on all data comprised in the BGI data base. The data have been retrieved among others in the campaigns of Ebblin (1983), Malinconico (1986) and Caporali (1993). The exact location of the measuring points is marked in the map with a dot. The non-homogeneous distribution of the dots is due to the highly inaccessibility of the area, which leads to limiting the measuring points greatly to the valleys. To the south of the MMT the anomalies stabilise to a lesser value of -200 mGal. In Kohistan and Southern Karakorum the isoanomales run parallel to the directions marked by the geologic structures, as the MMT and the Indus valley to the East. The gravity profiles AA' and BB' were obtained by projecting all gravity measurement locations with distances less than 50 km along the profiles. The data were gridded with a sampling distance of 5 km,

applying a weighted mean of the data falling inside the grid step. The weights were set equal to the inverse distance of the measurement location from the profile. The geographical co-ordinates are: A (33.545°N, 72.296°E), A' (36.954°N, 75.463°E), B (33.545°N, 72.269°E), B' (36.225°N, 72.315°E). The profiles were chosen so as to cut the gravity isolines orthogonally, as far as the data availability allowed it. The extension of profile AA' is 480 km, whereas the profile BB' is 300 km long. The greatest anomalies are found to the Northeast with values up to -560 mGal.

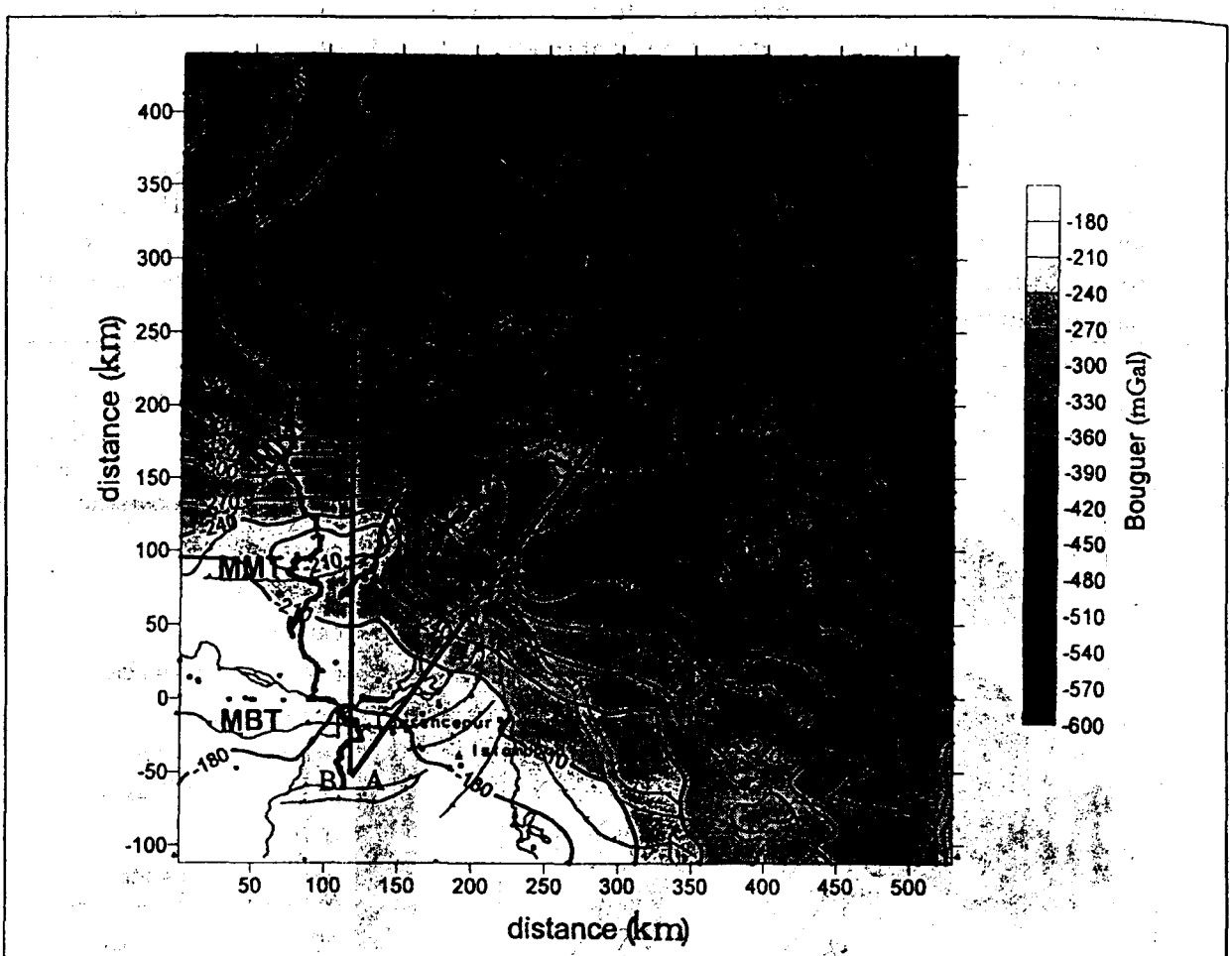

Fig. 3 Bouguer gravity map. Gravity data furnished by the BGI (Bureau Gravimetrique International)

Methodology

We consider the problem of inverting a series of sampled Bouguer gravity b(i) data (for i=1,N) along a profile in terms of the the crust-mantle density contrast. The inversion method we propose is the generalization of an inversion scheme published in Braitenberg et al., (1997), where the method is extensively explained and tested on synthetic models for the modelling of the Moho undulation. The method combines the downward continuation and the classical gravity field calculation of a mass distribution in an iterative scheme. Two parameters, the depth (d) and the density contrast ($\Delta\rho$) are required: the downward continuation implies the choice of the depth (d) at which the anomalous mass distribution is set. The interpretation of the flat mass distribution in terms of crustal inhomogeneities or oscillations of discontinuity level requires the assignment of the density contrast, defined as the difference between the densities above and below the discontinuity. The initial values for

the depth and the density contrast can be obtained in many cases from other geophysical sources as seismology or seismic sounding. As will be shown in the following, the correct depth can furthermore be determined during the inversion. In the case the crustal anomalies are seated at different depths in the same crustal column, the inversion is applied in successive steps, each pertaining to one source depth. Applying spectral methods the observed gravity field is divided into regional, medium and local field, these pertaining to deep, medium or superficial crustal bodies respectively. In several geophysical cases we can expect the depth and density contrasts to vary along the profile which leads to a series of reference depths (d_m, m=1,M) and density contrasts ($\Delta\rho_m$, m=1,M) between the positions x_m and x_{m+1} (m=1,M) along the profile (Fig. 4).

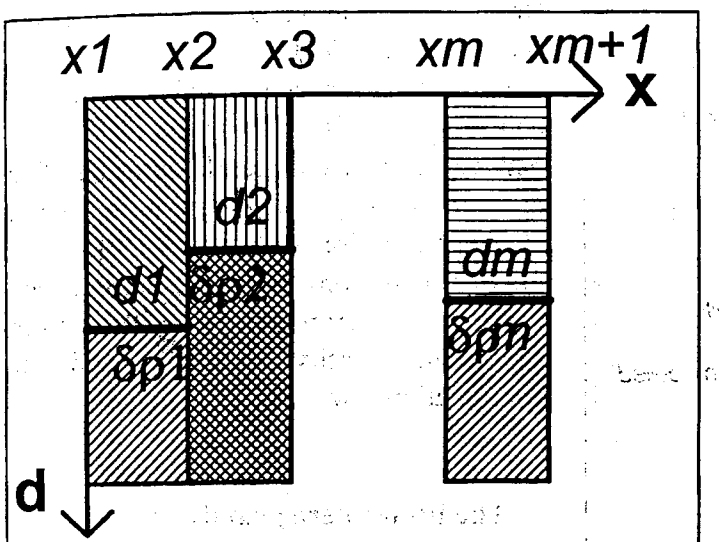

Fig. 4 Starting model used for the iterative downward continuation: a set of plane masses set at depth d_i having density contrast $\delta\rho_i$. The density contrast $\delta\rho_i$ is equal to the difference between the densities above and below the boundary

The inversion method is an iteration of two distinctive steps, illustrated in the flowchart depicted in Fig. 5.

The two steps are explained in the following. In the first iteration step set iter=1, in the second iter=2, and so on:

step (1) : We assume that the mass responsible for the residual (for iter=0, the Bouguer anomaly) $\delta g_{iter-1}(i)$, i=1,N is located at the depths d_m, m=1,M. The density contrast at the depth d_m is supposed to be $\Delta\rho_m$, the difference between the densities below and above the level d_m. The undulation of the discontinuity at depth d_m is calculated by applying the downward continuation law (Heiskanen and Moritz, 1967; Tsuboi, 1983; Zadro, 1986; Santero et al., 1988) as follows:

$$F_{iter}(j) = FT\left[\delta g_{iter-1}(i)\right] \qquad j=1,N$$

$$h_{iter}(i) = FT^{-1}\left[F_{iter-1}(j)\exp\left(k_j d_m\right)\right] / 2\pi G\Delta\rho \qquad i_m \le i \le i_{m+1},\ \text{for } m=1,M$$

$F_{iter-1}(j)$, j=1,N is the Fourier expansion (FT) of $\delta g_{iter-1}(i)$, i=1,N at resolved wavenumbers k_j, $h_{iter}(i)$, i=1,N is the calculated undulation, and G is the universal gravitational constant.

The anomalous crustal body is defined by the boundaries:

$$r_{iter}(i) = r_{iter-1}(i) + h_{iter}(i) \qquad i=1,N$$

and the levels d_m, $m=1,M$

At commencement of the iterations the boundary $r_0(i)$ is defined as:

$$r_0(i) = d_m \qquad i_m \le i \le i_{m+1} \qquad \text{for all } m=1,M$$

step (2) : The Newtonian gravitational effect of the crustal anomalous body defined by the undulation of the discontinuity $r_{iter}(i)$, i=1,N is computed at geoidal level, following classical methodologies (Nagy, 1966). The undulation is discretized and approximated by a finite number (K) of rectangular horizontal prisms of width (w). The residual gravity ($\delta g_{iter-1}(i)$, i=1,N) is obtained by subtracting the gravitational effect of the prisms from the observed Bouguer anomaly.

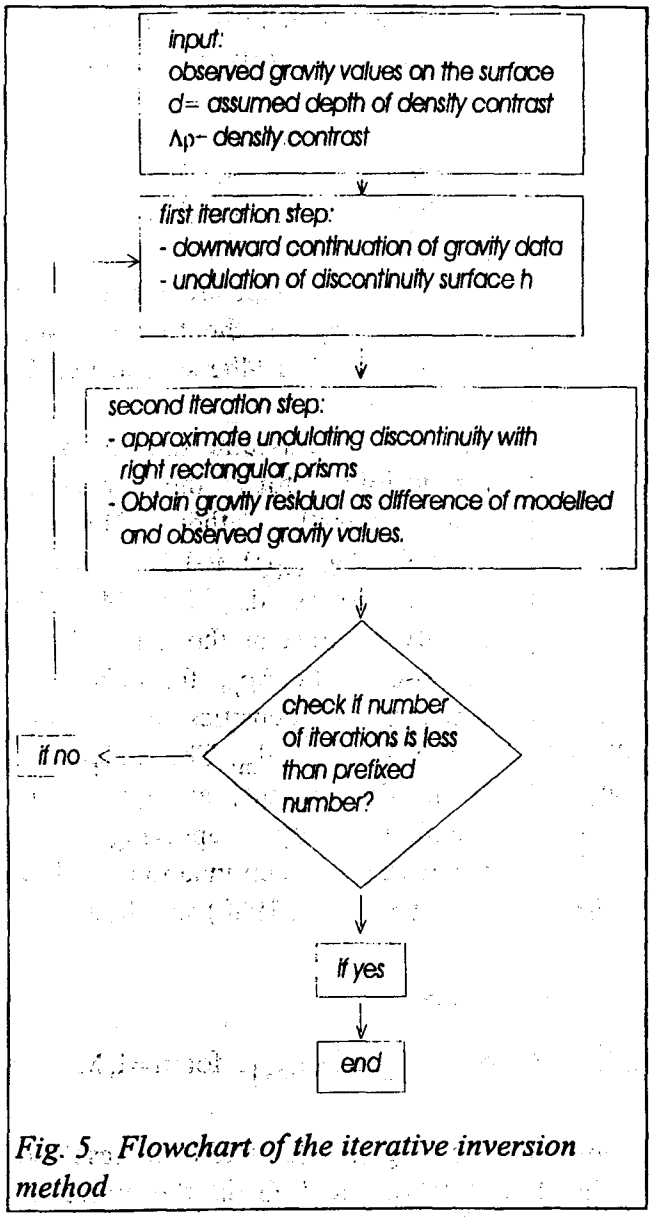

Fig. 5 - Flowchart of the iterative inversion method

The above method has been tested on synthetic models for the modelling of the Moho undulation and discussed in Braitenberg et al. (1997). In this case we set M=1. The depth (d_1) coincides with the mean Moho level and the density contrast ($\Delta\rho_1$) is equal to the difference between crustal and mantle densities. The observed gravity field is low-pass filtered at every iteration step, so as to free the gravity field from high spatial frequency variations, originating both from superficial density anomalies and the continuation law.

The lithosphere gravity effect

The low-frequency component of the Bouguer anomaly is mainly due to the undulations of the Moho. A small component may nevertheless be caused by lithospheric thickening. Presently, to our knowledge, the lithospheric structure in this area has been studied scarcely by seismological methods. An estimate of the lithospheric structure has been evaluated using lithospheric flexure models (Caporali, 1995). There are some uncertainties regarding the equivalence between the elastic thickness of the thin plate model and the thickness determined by seismological methods, but presently we do not have a more accurate source to estimate the gravimetric contribution of the lithosphere thickening in this area. The lithosphere results to range from a thickness of 90 km to a thickness of 120 km below the greatest topographic elevations. We model the lithosphere thickening with vertical rectangular prisms, assigning them the density contrast of lithosphere to asthenosphere (0.03 g/cm^3) given in Suhadolc et al. (1990). The gravity effect along the two profiles AA' and BB' of each prism is calculated with the classical procedure of Nagy (1966). The lithosphere gravity effect along the profiles AA' and BB' is shown in Fig. 6a and 6b, respectively. In the same graph the observed gravity along the profiles is given, at the same scaling. According to this lithosphere model the, gravity effect due to lithosphere

thickening is neglectable with respect to the observed Bouguer anomalies, and is not taken account in the course of the further analysis.

The crustal root from gravity inversion

Following the methodology exposed above, we approach the problem of determining the Moho-undulation along the two profiles AA' and BB'.

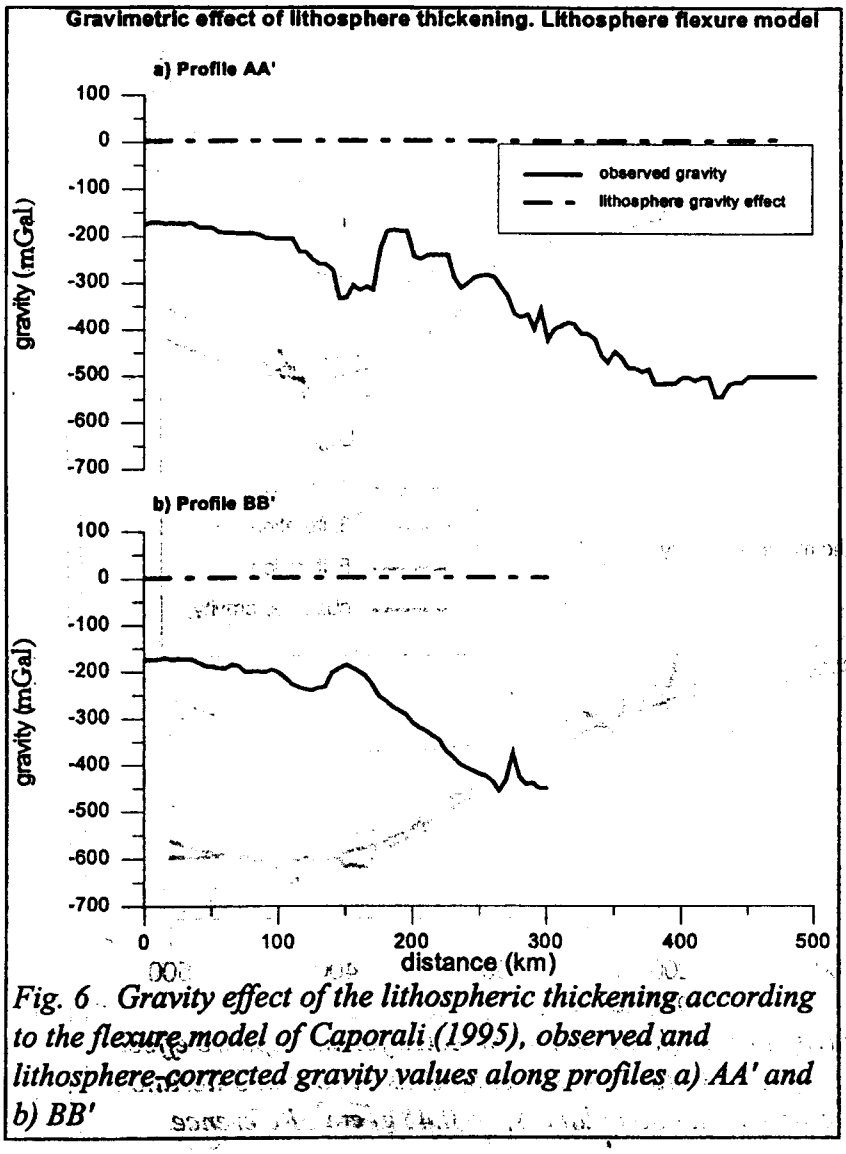

Fig. 6 . Gravity effect of the lithospheric thickening according to the flexure model of Caporali (1995), observed and lithosphere-corrected gravity values along profiles a) AA' and b) BB'

As we assume the presence of one single density boundary set at depth (d) with a density contrast ($\Delta\rho$), in this case M=1. The gravity data are padded with constant values at both ends to an extension of 1275 km. This eliminates border effects, which appear during analysis and enhances spectral resolution. We adopt the density contrast between crust and mantle proposed in Duroy et al. (1989) and in Lyon-Caen and Molnar (1983) as the most probable ($\delta\rho$=0.45 g/cm^3). The starting crustal thickness d is allowed to vary between 30 km and 40 km at steps of 5 km. The low pass filtering of the gravity data is performed in the frequency domain. The transfer function of the filter is a Hamming window, with cosine decrease for wavelengths down to 200 km, and zero values for shorter wavelengths. The number of iterations is fixed at 5, after which nearly no decrease in the gravity residual is obtained. The comparison of the calculated Moho depths with those obtained from seismics in the intersection points (Beloussov et al., 1983; Finetti et al., 1983) allows to anchor the curves to the correct depth, leading to a value of d (d=35 km). The crustal root is discretized in step (1) of the iterations with horizontal prisms of 20 km width, extending to a length of 10000 km to either side of the profile. The height of the prisms is set equal to the mean (over the 20 km width of the prism) deviation of the crustal root from the assumed reference depth (d).

In Fig. 7 the results obtained in the inversion steps are shown for profile AA'. The crustal root at different iteration steps is shown in Fig. 7a, the observed and modelled gravity in Fig. 7b. The crustal root has a depth of about 43 km in the southern end of the profile, gently increasing to 48 km at mark 200 km of the profile. The root steeply plunges from this

point to a maximum depth of 70 km at mark 410 km, after which it gently shallows toward the northern end of the profile. The successive iteration steps affect particularly the extension of the deepest part of the crustal root. At completed iteration the long period component of the observed gravity is reproduced well.

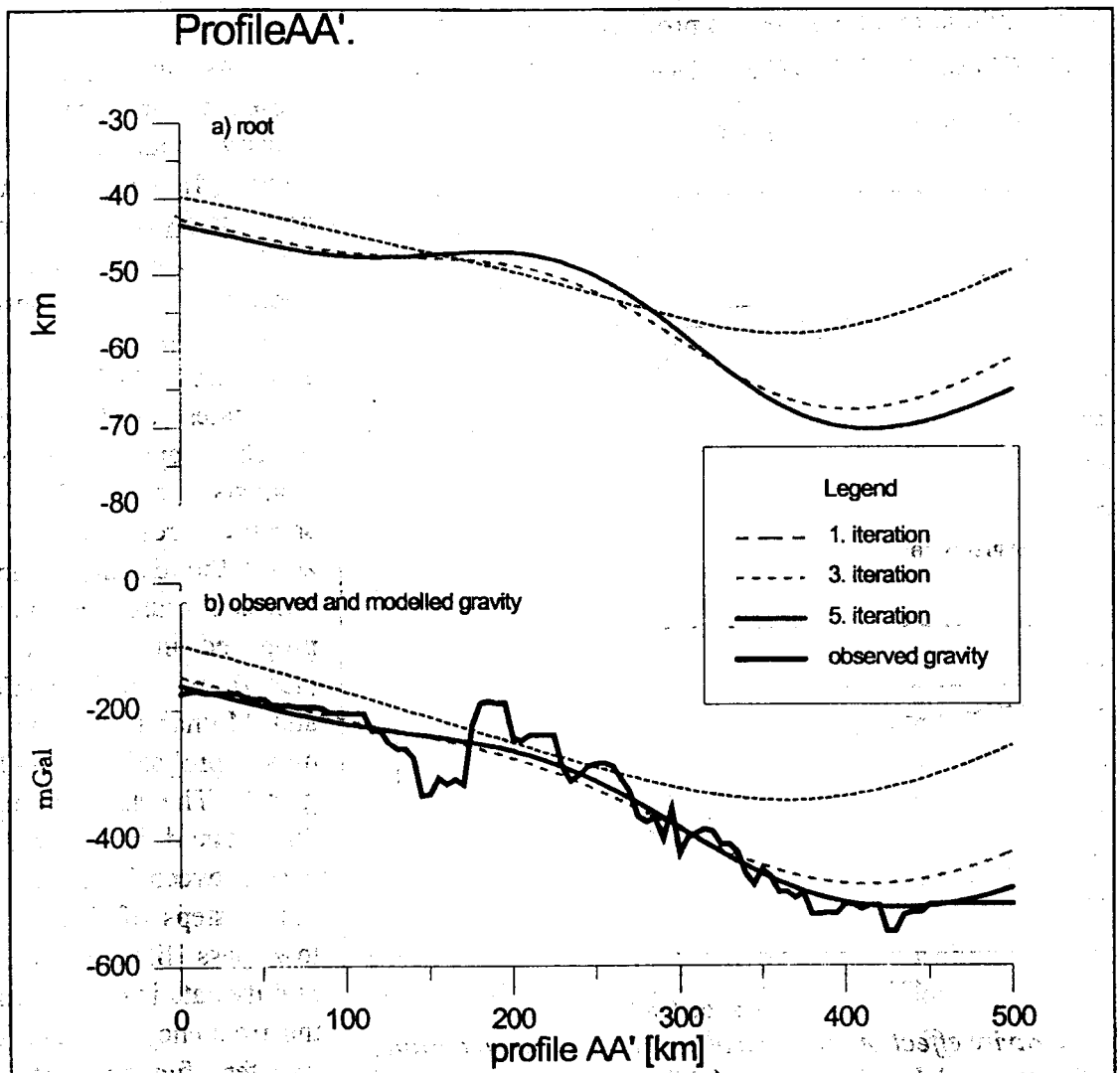

Fig. 7 Profile AA': a)gravity profile (heavy line) corrected for lithosphere effect and model gravity (dashed line) at 3 iteration steps. b) Crustal root at 3 iteration steps. Density contrast at crust-mantle boundary $\Delta\rho = 0.45$ g/cm^3. Reference crustal thickness d=35 km

In Fig. 8a,b the results of the inversion are shown for profile BB'. In the Southern part of the profile (mark 0 km) the crustal depth is comparable to that of profile AA' (40 km). At mark 150 km the depth steeply decreases down to the value of 65 km at the northern extreme of the profile.

Interpretation of the S-shaped gravity residual

The residual gravity is given in Fig . 9a and b, together with the local geology, for the two profiles. The residual gravity is the expression of the existence of anomalous masses at mid crustal or superficial depths. The dominant feature of the gravity residual for profile AA' (Fig. 9a) is an S-shaped anomaly with an impressive 160 mGal peak to peak amplitude. Also

for profile BB' (Fig.9b) the gravity residual reveals the S-shaped figure. The peak to peak amplitude is lower in this case (100 mGal). A sharp gravity high of 60 mGal is observed towards the northern end of the profile. The most remarkable feature in the gravity residuals of both profiles is the S-shaped anomaly, which we attempt to interpret in the present paragraph. First we localise the anomaly with respect to the local geology, following the geologic map edited by Tahirkheli (1983) (Fig. 2). The anomaly is positioned for both profiles on the intersection with the MMT. The positive part of the anomaly resides to the north of the MMT: qualitatively, it may be explained by the presence of the high-density rocks as the Jijal ultramafics and the Kamila Amphibolites. A first estimate of the densities of the rocks may be obtained from existing tables reporting the mean densities of different rock types. In table I the densities for the principal rock units are given, refering to the values published in Holbrook et al. (1992).

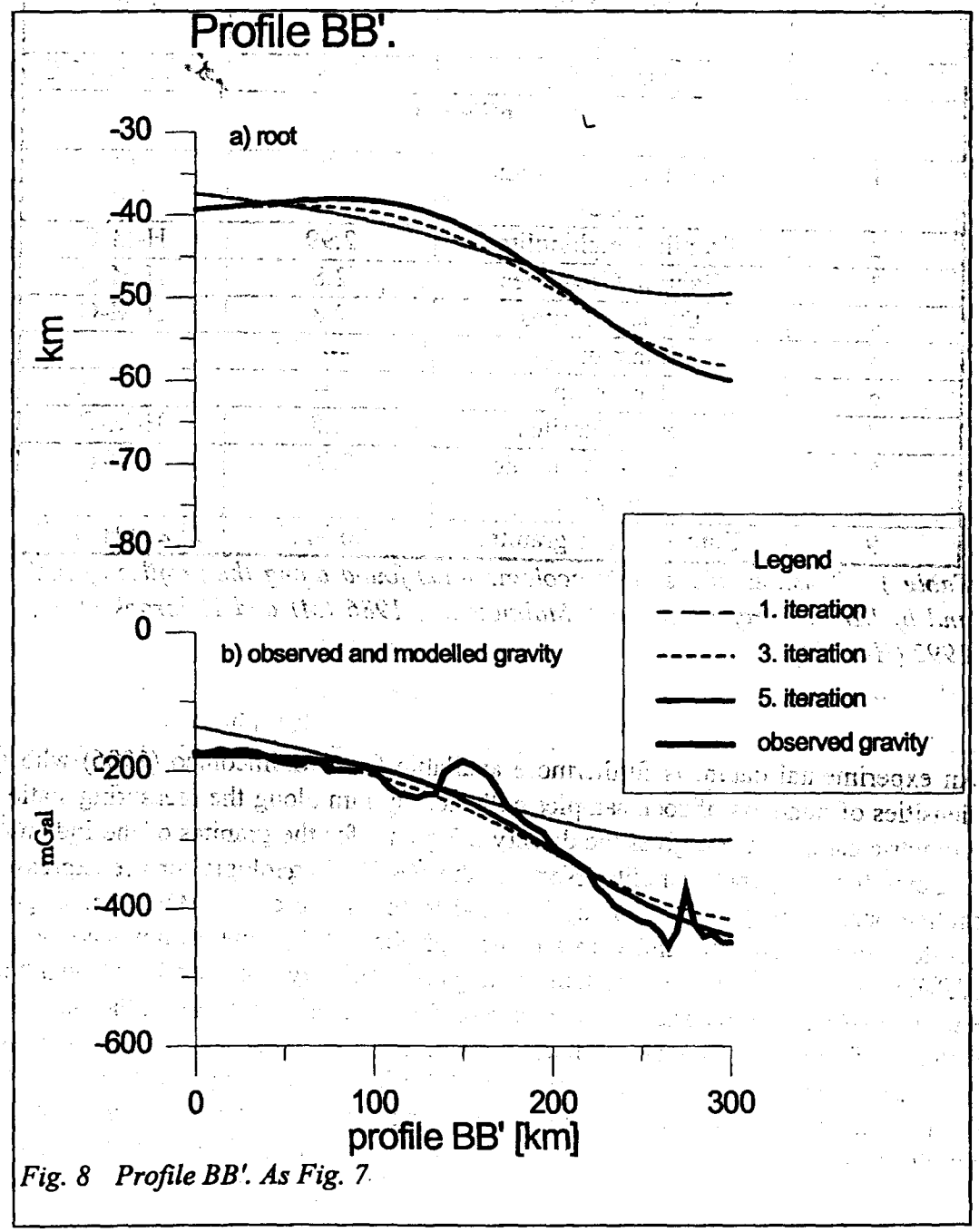

Fig. 8 Profile BB'. As Fig. 7

numeral of geologic unit in Figure	Composition	Density (g/cm^3)	Reference for density values
a) Profile AA'			
1	Granites	2.7	M
2	Jijal Ultramafics	3.2	M
3	Kamila Amphibolites	2.99	H-M-C
4 and 5	Bahrain Pyroxene Granulites	2.8	H-M-C
6	Deshai Diorites	2.8	H-M-C
7 and 8	Ladakh Intrusives	2.9	H-M-C
9	Rakoposha volcanic complex	2.91	H-M-C
10	Batholith	2.66	M and H-M-C
b) Profile BB'			
1	Para orthogneiss (Indian plate)	2.73	M
2	Kamila Amphibolites	2.99	H-M-C
3	Bahrain Granulites	2.8	H-M-C
4	Deshai Diorites	2.8	H-M-C
5	Kalam group	----	
6	Dir group	----	
7	Deshai Diorites	2.8	H-M-C
8	Rakaposhi Volcanic Complex	2.91	H-M-C
9	Eurasian plate granites	2.67-2.7	M and H-M-C

Table 1 Densities of the main geologic units found along the profiles a) AA' and b) BB'. The references are: Malinconico, 1986 (M) and Holbrook et al., 1992 (H-M-C).

An experimental datum is furthermore available from Malinconico (1986) who gives mean densities of hunderts of rock samples collected by him along the measuring stations of his gravimetric campaign. He gives the density 2.7 g/cm^3 for the granites of the Indian plate, and 3.2 g/cm^3 for the garnet granulites North of the MMT. No geologic surface expression of the negative part of the gravity anomaly is found to the South of the MMT. Infact granites cover uniformly a broad area, and with a density of about 2.7 g/cm^3 cannot account for the negative anomaly. We must conclude that the negative anomaly is caused by a down welling of upper or lower crustal material in the course of the subduction process of the Indian plate. The S-shaped figure may thus be modelled by two bodies, one set at mid to lower crustal depth, the other one cropping out at the surface. Referring to a two-layer reference crust with upper crustal density ρ_{cu} =2.7 g/cm^3 and lower crustal density ρ_{cl} =2.95 g/cm^3, the density contrast of the mid-crustal body is 0.25 g/cm^3. Assigning the surface body the density of amphibolites (3.0 g/cm^3) we obtain a density contrast for the outcropping body of 0.3 g/cm^3.

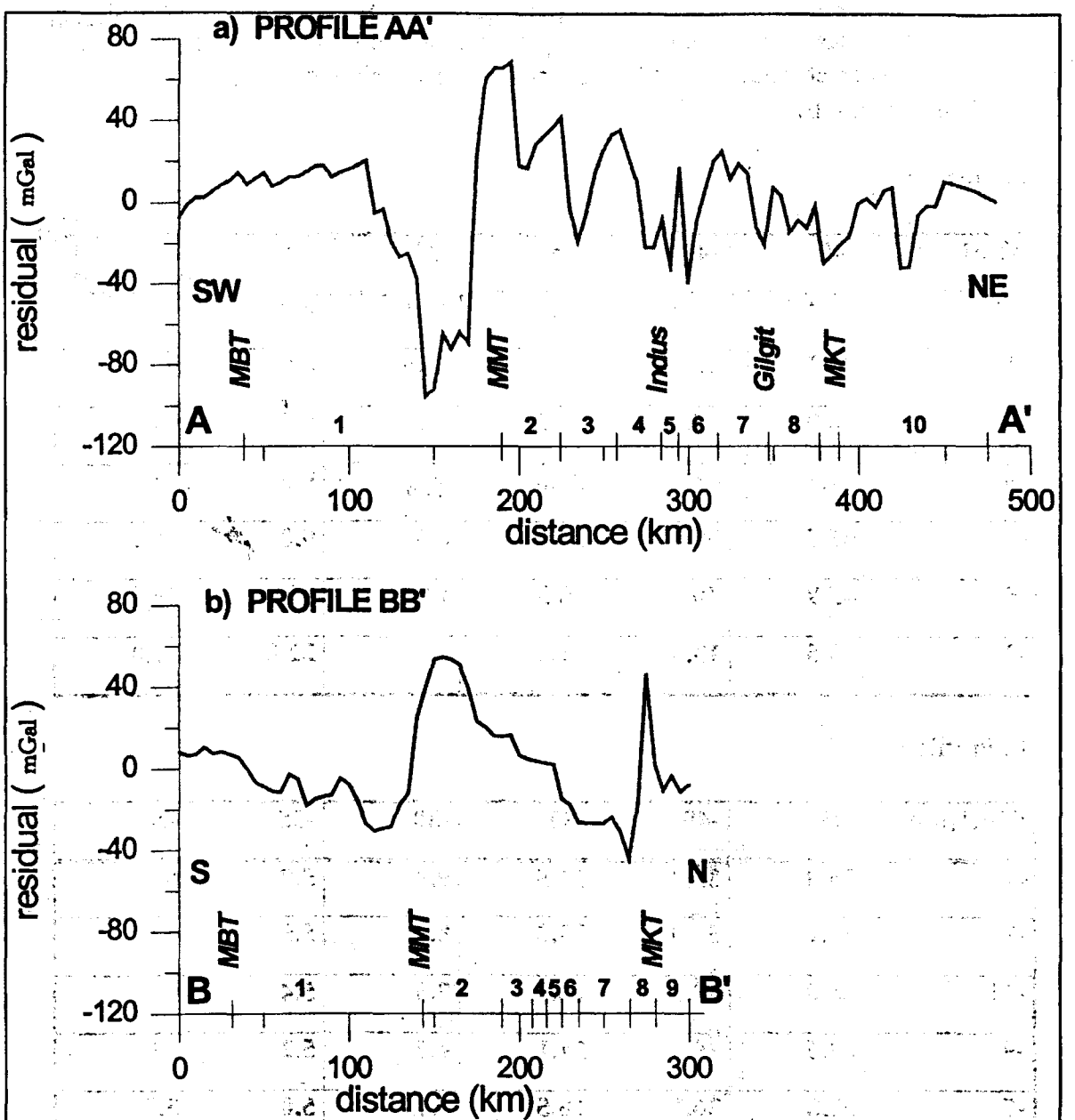

Fig. 9 . The gravity residual and the geologic units along the profile (Tahirkheli, 1983). a) Profile AA'. b) Profile BB'

We adopt the two-level continuation method explained in the previous paragraph, for estimating the sizes and depths of the two bodies. As in the long period inversion the analysed data extend to a total length of 1275 km, in order to eliminate border effects in the section of interest, which is 480 km long for AA' and 300 km for BB'. The data are low pass filtered in the frequency domain. The transfer function is a Hamming window, with cosine decrease for wavelengths down to 50 km, and zero values for shorter wavelengths. The smoothed gravity residual shown in Fig. 10a and 11a for the profiles AA' and BB', respectively (heavy continuous line). The position of the zero-passage of the S-shape is taken as dividing point between the two depths d1 and d2, at which the equivalent sheet mass distributions are set. We let d1 and d2 vary between geophysically acceptable limits (d1:

20km...45km; d2: 3km...15km) and calculate the root mean square gravity residual after five iterations for each case. The couple of d1, d2 for which the rms gravity residual is least, is accepted as the correct value. In table 2 the rms gravity residuals are given for profile AA' (Tab. 2 a) and profile BB' (Tab. 2 b).

a) Profile AA'

d2/d1(km)	-45	-40	-35	-30	-25	-20
-15	84.4	68.0	45.6	15.5	8.7	9.6
-13	78.3	62.5	36.2	12.0	8.8	9.7
-11	70.9	55.1	27.2	9.7	8.9	9.8
-9	64.2	48.3	20.0	**8.4**	9.0	9.9
-7	55.5	39.5	14.6	8.6	9.0	10.2
-5	45.9	30.2	15.3	13.2	11.6	20.1
-3	15.6	13.3	11.8	10.6	22.0	31.0

b) Profile BB'

d2/d1(km)	-45	-40	-35	-30	-25	-20
-15	25.0	35.4	37.5	9.3	5.7	6.3
-13	25.1	33.0	33.2	8.1	5.5	6.2
-11	28.0	31.1	28.7	7.3	5.4	6.0
-9	29.5	29.4	24.1	6.7	5.2	5.9
-7	32.8	26.1	18.5	5.7	5.0	5.7
-5	25.5	19.2	12.0	5.0	**4.8**	11.1
-3	7.7	6.9	6.1	5.6	12.7	11.3

Table 2 Standard deviation of the rms gravity residual for different values of the reference depths d1 and d2 from the inversion of the S-shaped anomaly. a) Profile AA'. b) Profile BB'

For profile AA' the residual is minimal for the lower depth d1 of 30 km, for profile BB' we find the depth of 25 km. The depth of the superficial body resumes to 9 km and 5 km for profiles AA' and BB', respectively. The oscillations of the two density boundaries obtained from the two-level iterative version are shown in Fig. 10b and 11b. An oscillation of the boundary above the reference depth indicates the presence of a surplus mass, whereas an oscillation below the reference depth is due to a mass deficit with respect to the reference

crustal column. To the North of the MMT the boundary reaches the surface, which is interpreted as high density material cropping out. The deepening of the boundary to the South of the MMT is very pronounced for profile AA', and goes down to depths which lie below the Moho. This result is of difficult geophysical interpretation. The maximum depth-extension of the body could though be exaggerated due to the limited spectral components used for constructing the root. This implies that steep flanks cannot be correctly modelled, wherefore the inversion process deepens the root in order to accomplish the given gravity anomaly. Furthermore this model does not account for inclined structures.

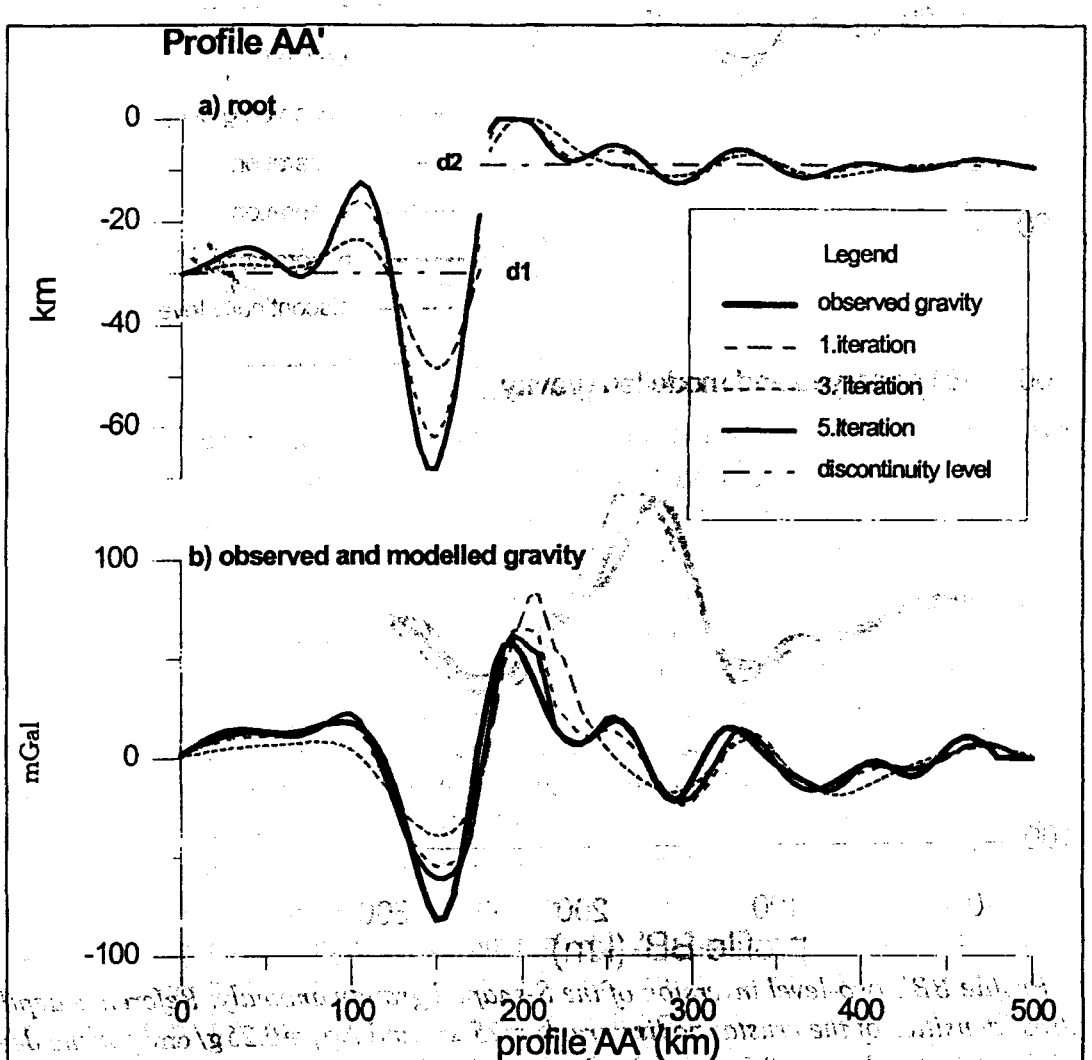

Fig. 10 Profile AA': two-level inversion of the S-shaped gravity anomaly. Reference depths and contrast densities of the crustal bodies are d_1 =30 km and $\Delta\rho_1$ =0.25 g/cm^3 for the deep body and d_2 =9 km and $\Delta\rho_2$ =0.3 g/cm^3 for the superficial body

The results from this inversion should be used as starting values in a successive procedure, which considers the modelling with vertical or inclined prisms. It is nontheless interesting that the position of the body is in correspondence with the IKSZ found by Ambruster et al.

(1978). The maximum depth-extent of the seismicity along the IKSZ reaches 70 km. It seems thus that the margins of the low-density body are signed by a seismic zone.

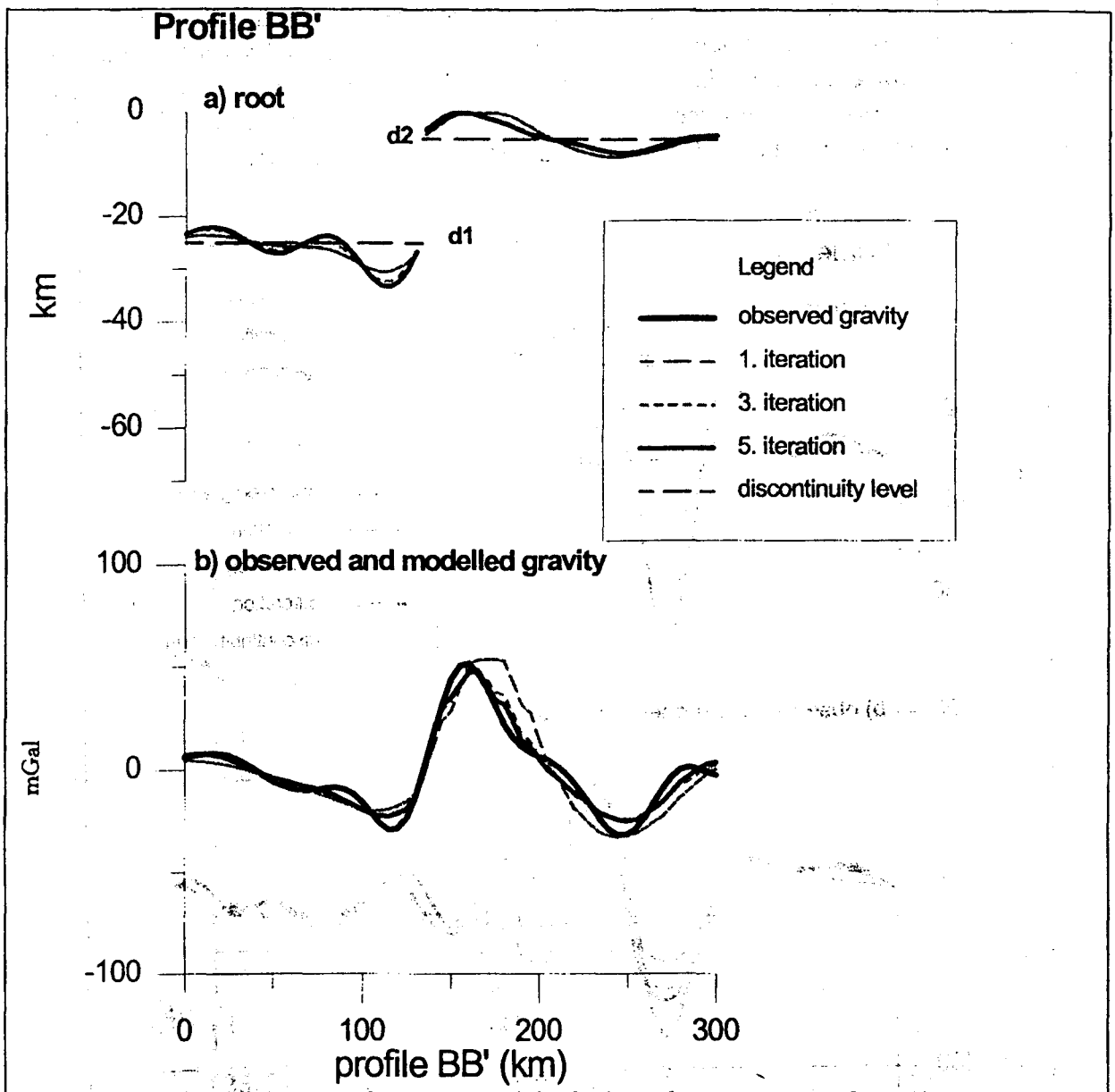

Fig. 11 Profile BB': two-level inversion of the S-shaped gravity anomaly. Reference depths and contrast densities of the crustal bodies are d_1 =25 km and $\Delta\rho_1$ =0.25 g/cm^3 for the deep body and d_2 =5 km and $\Delta\rho_2$ =0.3 g/cm^3 for the superficial body.

Discussion and conclusion

The simple down/upward continuation gives an exact estimate of the relation of the gravity field at the surface and the mass distributions at depth, in the case that the mass distribution is flat. If then the flat distribution is expanded into an oscillating boundary, as is done for a density discontinuity, the upward continued field only gives a first estimate of the gravity field. With our method the oscillation of the density boundary is corrected iteratively, until the residual between the gravity field it produces and the starting gravity field is minimal. The method can be applied profitably in different model situations; one important application considers the inversion of the Moho, taking advantage of the strong density contrast between the lower crust and upper mantle. In the SE Alps the "gravity Moho" was

thus obtained and its deviation by several km from the isostatic root could be shown. The resulting depths were in excellent accordance with the values furnished in some intersection points by DSS (Braitenberg et al., 1997). A further application could be a laterally varying density contrast along a defined depth, as we can imagine across a rift zone. In the present study we complicate the model a step further, allowing also the density boundary depth, next to density, to vary along the profile. We have tested the methodology on a synthetic model which was made of a crustal deep root and a superficial high density body representing a crustal flake overthrust to the surface. The inversion procedure could retrieve the synthetic model well. The criteria of minimizing the rms gravity residual permitted to select the correct values for the depths of the density contrasts. The rms residual was also tested for retrieving the density contrasts assumed, but is less sensible to this parameter. It follows that in the geophysical case, it is convenient to estimate the density contrast from geological assumptions or seismological velocity crustal models.

The above inversion scheme has found a twofold application in the inversion of the gravity field in the Karakorum in NE-Pakistan. The area is gravimetrically interesting owing to its extremely high negative Bouguer anomalies. The inversion was separated into two steps: the first regarding the inversion of the long period gravity variation interpreted as the oscillation of the Moho-boundary, the second the inversion of the residual field, having its origin at superficial to mid crustal depths. This under the assumption that the spectrum of the gravity field reflects the depth of the sources, the deep sources affecting the low spatial frequencies, the superficial sources the high frequencies. The Moho depths we obtain generally agree well with those determined with other geophysical methods. A deepening of the Moho, as expected, is found from the Indian foreland across the Kohistan Arc in a NE-direction. The deepest values reach 70 km just North of the Indus suture (MKT). It is interesting that below the surface expression of the MMT, a flattening of the Moho is observed. Theoretical lithospheric flexure models assume in this area the contact of two distinct lithospheric plates, the Indian plate to the South, and the European plate to the North (Caporali, 1995). The gravity residual for this crustal model has for both profiles a characteristic negative-positive anomaly couple. It resembles the anomalies described by Karner and Watts (1983) as typical for mountain ranges. One main difference is that in our case the geographical extension of the low-high couple is limited to about 150 km. The authors Karner and Watts (1983) interpret the anomaly couple as evidence of subsurface (buried) and surface (topographic) loading. Fountain and Salisbury (1981) describe a similar characteristic gravity anomaly in a more specific situation and define it distinctive for exposures of continental crust along great faults during continental collision. The case we describe agrees with both of the above proposals: the presence of the ultramafics at the MMT and the geological sequence to the North of the MMT has been interpreted as an exposure of the lower crust of the Kohistan Island Arc (Tahirkheli, 1983). The positive part of the gravity couple can thus be explained by the presence of high density surface rocks cropping out at the surface. Our inversion method gives a thickness of the outcropping high density body of 7 km. The gravity low has no corresponding surface expression sediments and cannot be explained by crustal thickening alone, due to its steep flanks. Applying our inversion method we find that the negative part of the anomaly is explained by a low density body with its top at mid-crustal depths, and reaching the Moho or even greater depths. This last body would confirm the proposal of Karner and Watts (1983) of associating the positive-negative couple to subsurface bodies. The low density body can be interpreted as being made of a lighter upper crust flexed or folded down to depths of the lower crust, and the lower crust flexing into the mantle. The downward flexure of the Indian crust had been proposed by Duroy et al.

(1989) in their flexure model of the Indian plate. Unfortunately it can presently not be verified, how far the positive-negative couple extends along the MMT, due to the inaccessibility of the terrain and the resulting inhomogeneous distribution of the gravity data. It remains an open problem, whether the positive-negative couple is a local phenomenon characteristic of the exceptional position at the sharp bend of the MMT, or whether it is ubiquitous to this suture boundary.

Acknowledgements: Prof. M. Zadro assisted costantly at the progress of this work and gave numerous suggestions. This work was done with the financial contributions of CNR 96.00289CT05 Braitenberg.

References

Armbruster J., L. Seeber and K.H. Jacob (1978). The Northwestern termination of the Himalayan mountain front: active tectonics from microearthquakes. J. Geoph. Res., **83**, 269-282.

Beloussov V.V., B.S. Volvovsky, I.S. Volvovsky, K.L. Kaila, A. Marussi, H. Narain, B.B. TAl-Virsky, I. Finetti and I. Kh. Khamrabaev (1983). General features of the lithospheric structure of southern Tien Shan, the Pamirs, Karakorum and the Himalayas. Boll. Geof. Teor. Appl., **25**, 151-161.

Braitenberg C., F. Pettenati and M. Zadro (1997). Spectral and classical methods in the evaluation of Moho undulations from gravity data: the NE Italian Alps and isostasy. J. Geodynamics, **23**, 5-22.

Caporali A. (1993). Recent gravity measurements in the Karakoram, in Himalayan Tectonics, special pubblication 74 ed. by P.J.Treloar and M.P. Searle, 9-20, Geological Society London.

Caporali A. (1995).Gravity anomalies and the flexure of the lithosphere in the Karakoram, Pakistan. J. Geoph. Res., **100**, 15075-15085.

Coward M.P., B.F. Windley, R.D. Broughton, I.W. Luff, M.G. Petterson, C.J. Pudsey, D.C. Rex and M. Asif Khan (1986). Collision teconics in the NW Himalayas. in Coward, M.P. and A. C. Ries (eds.): Collision Tectonics, Geological Society Special Publication No. 19, 20-219.

Duroy Y., A. Farah and R.J. Lillie (1989). Subsurface densities and lithosheric flexure of the Himalayan foreland in Pakistan. 217-236. in: Malinconico, Jr. L.L. (ed.) Tectonics of the western Himalayas, Geological Society of America, Special Paper 232, 1-320.

Ebblin C., A. Marussi, G. Poretti, S.M. Rahim and P. Richardus (1983). Gravity measurements in the Karakorum. Boll. Geof. Teor. Appl., **25**, 303-316.

Farah A., M.A. Mirza, M.A. Ahmad and M.H. Butt (1977). Gravity field of the buried shield in the Punjab Plain, Pakistan, Geological Society of America Bulletin, **88**, 1147-1155.

Finetti I., G. Poretti and M.A. Mirza (1983). Crustal structure of the Karakorum range along the DSS profile Nanga Parbat-Karakul. Boll. Geof. Teor. Appl., **25**, 195-209.

Fountain D.M. and M.H. Salisbury (1981). Exposed cross-sections through the continental crust: implications for crustal structure, petrology, and evolution. Earth and Planetary Science Letters, **56** (1981), 263-277.

Heiskanen W.A. and H. Moritz (1967). Physical geodesy, pp. 249-250. W.H. Freeman and Co., San Francisco.

Holbrook W.S., W.D. Mooney and N.I. Christensen, (1992). The seismic velocity structure of the deep continental crust. In: Fountain D.M., Arculus R. and Kay R.W. (eds.): Continental lower crust, Elsevier, Amsterdam, 1992, pp. 1-43.

Karner G.D. and A.B. Watts (1983). Gravity anomalies and flexure of the lithosphere at mountain ranges. J. Geoph. Res., **88**, 10449-10477.

Lyon-Caen H. and P.Molnar (1983). Constraints on the structure of the Himalaya from an analysis of gravity anomalies and a flexural model of the lithosphere. J. Geoph. Res., **88**, 8171-8191.

Malinconico Jr. L.L. (1986). The structure of the Kohistan-Arc terrane in Northern Pakistan as inferred from gravity data. Tectonophysics, **124**, 297-307.

Malinconico Jr L. L. (1989). Crustal thickness estimates for western Himalaya. In: Tectonics of the western Himalayas (Editors: Malinconico L.L.Jr. & Lillie R.J.), Geol. Soc. of America (Special Paper, 232), 237-242.

Marussi A. (1976). Gravity in the Karakorum. In: International Colloquium on the geotectonics of the Kashmir Himalaya-Karakorum-Hindu Kush and Pamir orogenic belts, Accademia Nazionale Lincei, Rome, 131-137.

Marussi A. (1983). Geophysical trends and evolution of the Pamirs syntaxis and Karakorum. Boll. Geof. Teor. Appl., **25**, 443-461.

McGinnis L.D. (1970). Tectonics and the Gravity field in the continental interior. J. Geoph. Res., **75**, 317-322.

McGinnis L.D. (1971). Gravity and Tectonics in the Hindu Kush. J. Geoph. Res., **76**, 1894-1904.

Nagy D. (1966). The gravitational attraction of a right rectangular prism. Geophysics, **XXX**, 362-371.

Santero P., M. Zadro, D. Blitzkow and N.C. de Sa' (1988). Gravimetric analysis of the Goiana flexure, Northern Parana' Basin. In: The Mesozoic Flood of the Parana' Basin. Piccirillo E.M. and A.J. Melfi (eds.), pp. 257-270. Instituto Astronomico e Geofisico, Sao Paolo.

Suhadolc P., G.F. Panza and S.Mueller (1990). Physical properties of the lithoshere-asthenosphere system in Europe. Tectonophysics, **176**, 123-135.

Tahirkheli R.A.K.(1983). Geological evolution of Kohistan island arc on the southern flank of the Karakoram Hindu Kush in Pakistan. Boll. Geof. Teor. Appl., **XXV**, 351-364.

Tsuboi C. (1983). Gravity. pp. 110-121, 204-210. Allen & Unwin, London.

Verma R.K. and K.A.V.L. Prasad (1987). Analysis of gravity fields in the northwestern Himalayas and Kohistan region using deep seismic sounding data. Geophys. J.R.astr.Soc., **91**, 869-889.

Zadro M. (1986). Spectral images of the gravitational field. Manuscripta Geodaetica, **11**, 207-213.